Byung Ihn Choi
Editor

Radiology Illustrated
Hepatobiliary and Pancreatic Radiology

Springer

Byung Ihn Choi
Editor

Radiology Illustrated: Hepatobiliary and Pancreatic Radiology

Springer

Editor
Byung Ihn Choi
Department of Radiology
Seoul National University Hospital
Seoul
Republic of Korea

ISSN 2196-114X eISSN 2196-1158
ISBN 978-3-642-35824-1 ISBN 978-3-642-35825-8 (eBook)
DOI 10.1007/978-3-642-35825-8
Springer Heidelberg New York Dordrecht London

Library of Congress Control Number: 2013956429

Contents

Anomalies and Anatomic Variants of the Liver

1

Ijin Joo and Ah Young Kim

Contents

I. Joo
Department of Radiology, Seoul National University Hospital,
Seoul, Republic of Korea
e-mail: hijijin@gmail.com

A.Y. Kim (✉)
Department of Radiology, University of Ulsan,
Asan Medical Center, Seoul, Republic of Korea
e-mail: aykim@amc.seoul.kr

B.I. Choi (ed.), *Radiology Illustrated: Hepatobiliary and Pancreatic Radiology*, Radiology Illustrated,
DOI 10.1007/978-3-642-35825-8_1,

Knowledge of the anomalies and anatomical variants of the liver is often of great importance because these may be misinterpreted as pathologic conditions. While congenital anomalies of the liver are rare, anatomic variants are relatively common. The congenital anomalies of the liver include agenesis or hypoplasia of the hepatic lobes or segments, Riedel's lobe, and other accessory hepatic lobe. Anatomic variants contain accessory fissures and diaphragmatic slips, sliver of the liver, and variants related to papillary process of the caudate lobe.

1.1 Agenesis and Hypoplasia of the Hepatic Lobe or Segment

Agenesis and hypoplasia of hepatic lobes or segments are uncommon developmental anomalies. Agenesis is a condition of complete absence of hepatic lobes or segments, whereas hypoplasia is a condition which the size of a hepatic lobe or segment is relatively small but otherwise normal. The most commonly involved segments are the anterior segment of the right lobe and the medial segment (segment IV). Before making a diagnosis of agenesis or hypoplasia, it is important to exclude other causes of acquired atrophy of the hepatic lobes or segments, caused by cirrhosis, biliary obstruction, postsurgical resection, or rarely vascular compromise. In cases of agenesis, hepatic parenchyma as well as corresponding lobar or segmental vessels is absent, whereas at least one of those structures is detected in cases of acquired atrophy. Agenesis or hypoplasia of the hepatic lobes and segments may alter the normal topography of the upper abdomen, that is, change in position of adjacent organs such as the stomach, colon, or kidney.

1.2 Riedel's Lobe

Riedel's lobe is a downward, tongue-like projection from the anterior aspect of the right hepatic lobe. It is controversial whether Riedel's lobe is congenital or acquired in origin. Awareness of Riedel's lobe is clinically important since it is one of the causes of right-sided abdominal palpable masses on physical examination. However, correct diagnosis can be easily achieved by demonstrating of its connection with right hepatic lobe on imaging modalities. Riedel's lobe is usually asymptomatic. However, it can give rise to symptoms such as acute or intermittent abdominal pain if it is complicated by torsion.

1.3 Accessory Hepatic Lobe

Accessory hepatic lobe is a rare congenital anomaly and occurs from an error in the formation of the endodermal caudal foregut in the third gestational week and segmentation of the hepatic bud. It is composed of normal hepatic tissue and contains its own hepatic vessels and bile ducts. Most cases of accessory lobes are attached to the inferior surface of the liver by either a normal hepatic parenchyma or a mesentery. Occasionally, they have been found around gallbladder fossa, gastrohepatic ligament, umbilicus, adrenal gland, pancreas, esophagus, and rarely the thoracic cavity. Accessory hepatic lobes can mimic soft tissue masses or lymph nodes, but they can be differentiated from other pathologic condition by means of identification of their continuity with main liver on imaging modalities using multiplanar reconstruction. Although most accessory lobes are usually asymptomatic and found incidentally, some pedunculated ones may undergo torsion of their vascular pedicles.

1.4 Accessory Fissure and Diaphragmatic Slip

In addition to the major hepatic fissures such as fissures for falciform ligament and ligamentum venosum, the liver may contain accessory and pseudoaccessory fissures. True *accessory fissures* result from inward folding of the peritoneum; therefore, ascites may extend into these fissures or peritoneal pathology can be appeared. Accessory fissures are rare but relatively common in the undersurface of the liver. The most common one is the inferior accessory fissure, which is located in the surface of posterior segment of the right lobe. Invagination of the diaphragmatic muscle fibers results in *pseudoaccessory fissures*, usually along the superior surface of the liver. They are common anatomic variants and more frequently seen in the right hepatic lobe. These diaphragmatic slips can mimic hepatic nodules.

Differentiation of hepatic accessory or pseudoaccessory fissures from pathologic lesions may be achieved by a careful analysis of contours of the liver and diaphragm and by knowing the various findings of these variants. On CT scan, they can appear as hypoattenuated nodules in the peripheral portion of the liver. On ultrasound, they may be seen as echogenic nodular lesions in one plane. However, when scanning in the orthogonal plane, echogenic linear morphology may be revealed along the hepatic dome.

1.5 Sliver of the Liver

Leftward extension of the left lateral segment of the liver is referred to as "sliver of the liver." It is a common anatomic variant and appears as a crescent density which wraps around the spleen in the left upper quadrant abdomen. Knowledge of imaging features of this variant is important to not to confuse this portion of the liver for a pathologic condition originating from the stomach or spleen. This potential misdiagnosis can be avoided by demonstration of continuity between the "sliver of the liver" and the remainder of the left hepatic lobe.

1.6 Papillary Process of the Caudate Lobe

The caudate lobe is a medial extension of the right hepatic lobe between inferior vena cava and the fissure for ligamentum venosum. Occasionally, it is divided inferiorly into two processes: papillary and caudate processes. The *papillary process* extends medially and to the left in the region of the lesser sac, while the caudate process extends posteriorly. Papillary process of the caudate lobe can appear separate from the liver on some sections of the axial images; therefore, it can mimic an enlarged periportal lymph node or a soft tissue mass near the pancreas head. Serial axial images as well as multiplanar reformatted images are occasionally helpful for differentiating the papillary process form extrahepatic lesions.

1.7 Summary

1. Knowledge of the imaging features of anomalies and anatomic variants of the liver is important not to misinterpret these as pathologic conditions. Multiplanar reformatted images would be occasionally helpful to make correct diagnosis.
2. Riedel's lobe is one of the possible causes of abdominal palpable mass, and it can undergo torsion.
3. Accessory fissure of the liver is most commonly found in the surface of posterior segment of the right lobe.
4. Diaphragmatic slips are common pseudoaccessory fissures in the hepatic dome which result from invagination of the diaphragm.
5. Leftward extension of the left lateral segment of the liver (sliver of the liver) is a common anatomic variant which may mimic perisplenic mass.
6. Papillary process of the caudate lobe can mimic an enlarged lymph node or a soft tissue mass on axial images.

1.8 Illustrations: Anomalies and Anatomic Variants of the Liver

1.8.1 Illustrations of Normal Segmental Anatomy of the Liver

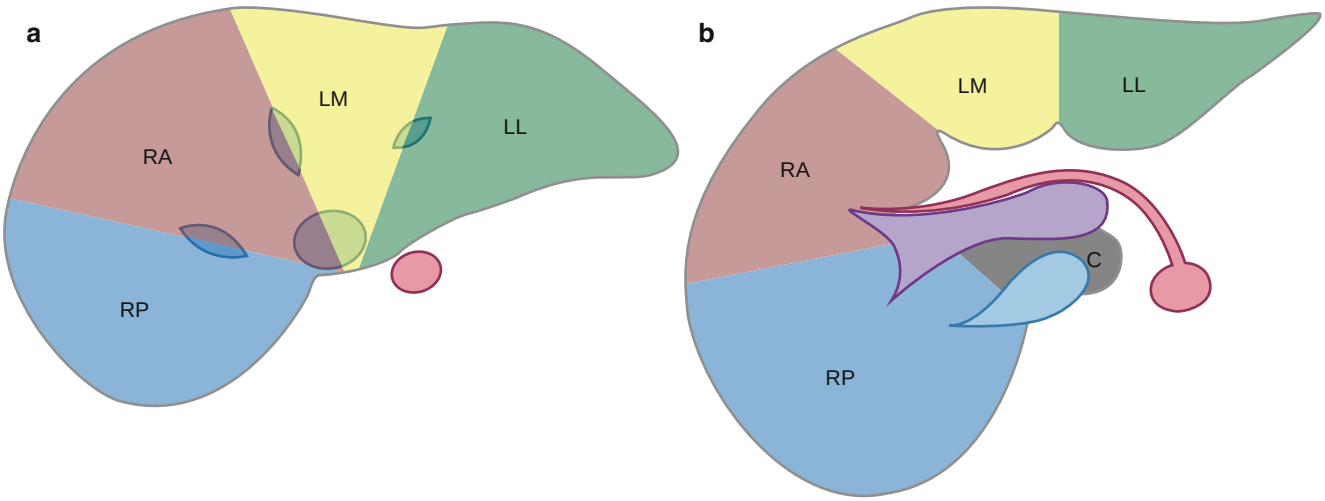

Fig. 1.1 Illustrations of normal segmental anatomy of the liver on cross-sectional images. (**a**, **b**) Segmental anatomy of the liver is usually determined by the portal vein branches and hepatic veins. Congenital anomalies such as agenesis and hypoplasia of hepatic lobes or segments alter the normal morphology which can be appeared as absence and relatively small size of lobes or segments. *RP* right posterior segment, *RA* right anterior segment, *LM* left medial segment, *LL* left lateral segment, *C* caudate lobe

1.8.2 Agenesis of the Right Lobe of the Liver

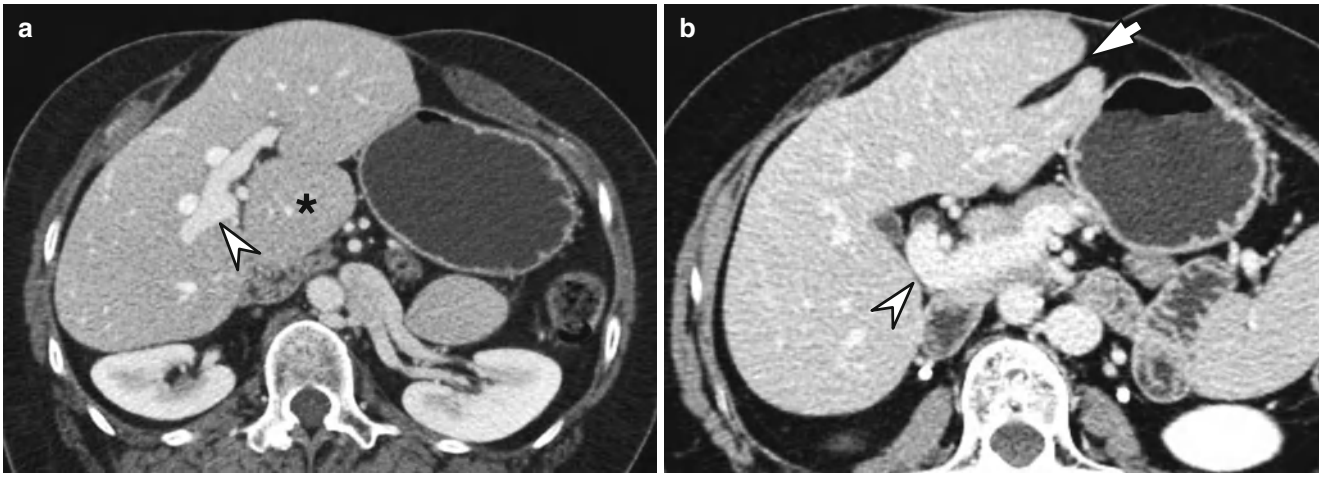

Fig. 1.2 Agenesis of the right lobe of the liver. (**a**) Axial CT image at the level of left portal vein shows bifurcation of the segmental portal branches from the umbilical portion (*arrowhead*) of the left portal vein. Note the absence of the right hepatic lobe and hypertrophy of the caudate lobe (*asterisk*). (**b**) CT image which is more caudal to (**a**) demonstrates the origination of the left portal vein (*arrowhead*); however, there is no vascular structure corresponding to right portal vein. Note the accessory fissure (*arrow*) in the left lateral segment

1.8.3 Agenesis of the Left Lateral Segment of the Liver

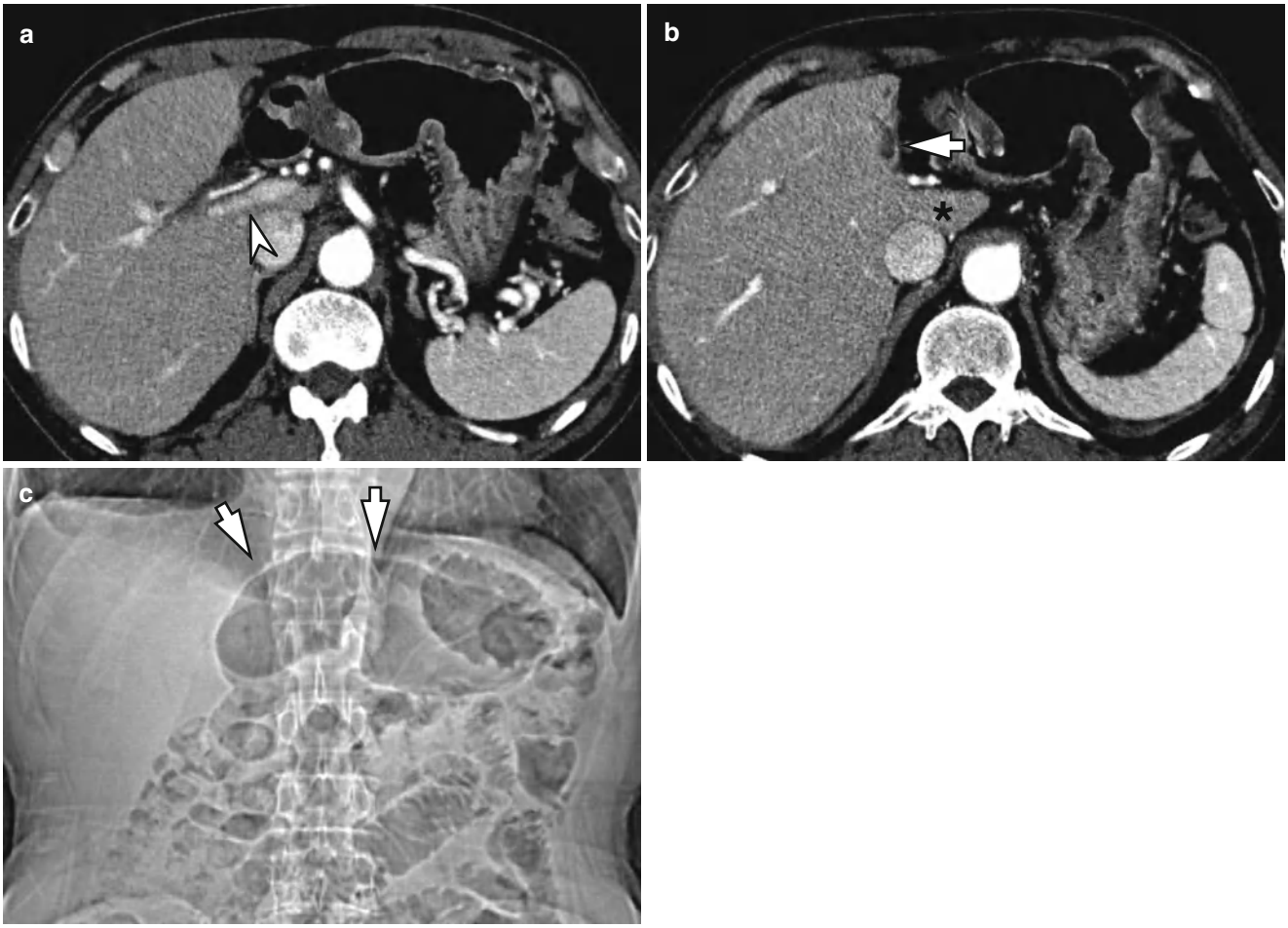

Fig. 1.3 Agenesis of the left lateral segment of the liver. (**a**) Axial contrast-enhanced CT reveals absence of left portal vein while right portal vein is present (*arrow*). (**b**) On the more cranial image, the left lateral segment is absent while the medial segment is supplied by middle hepatic artery (*arrow*) and caudate lobe (*asterisk*) is present. (**c**) Topogram shows transverse and high-positioned stomach (*arrows*)

1.8.4 Hypoplasia of the Left Lateral Segment of the Liver

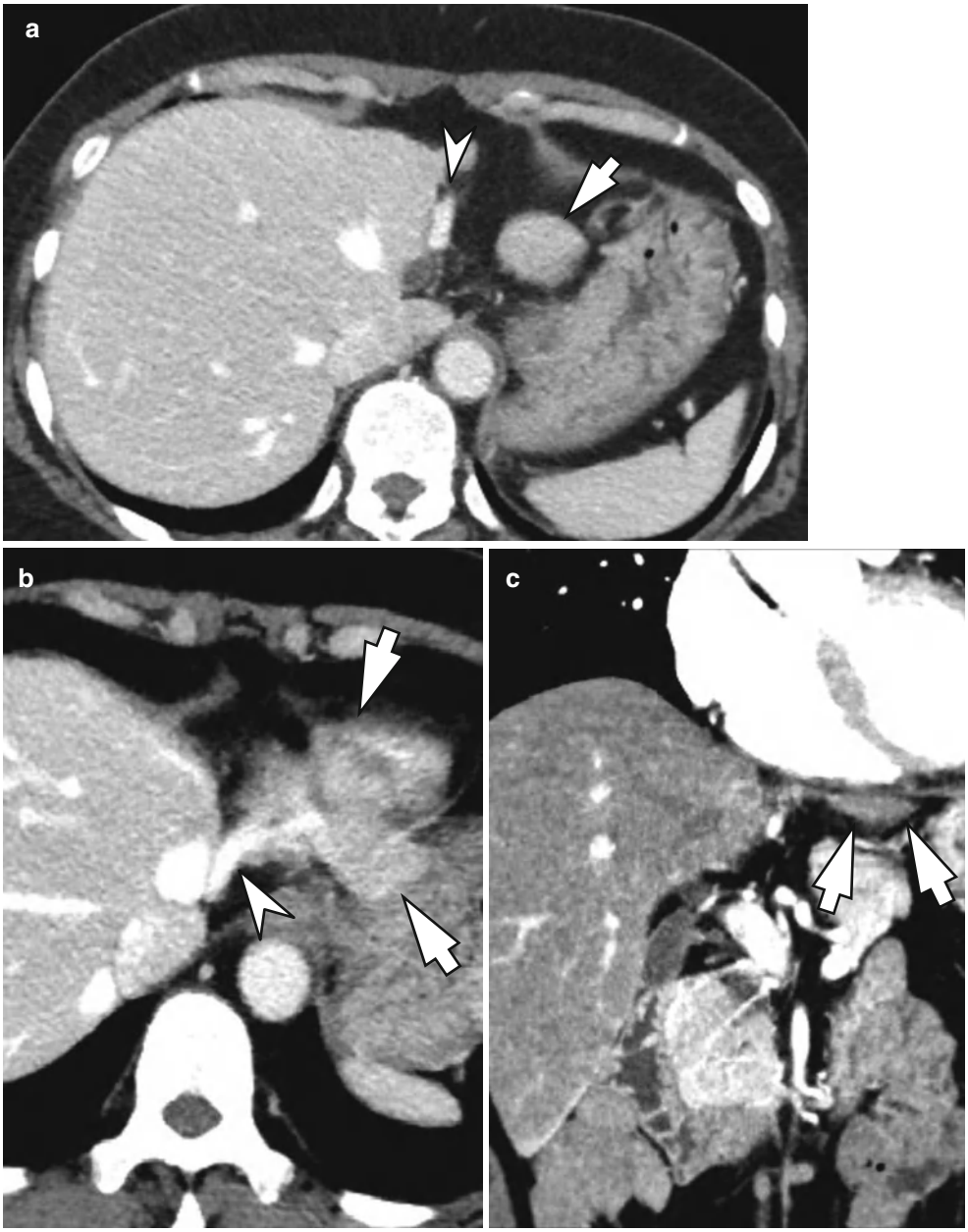

Fig. 1.4 Hypoplasia of the left lateral segment of the liver. (**a**) Axial CT image shows the hypoplastic liver tissue of left lateral segment (*arrow*) which mimics an enhancing soft tissue mass or lymphadenopathy of the perigastric space. Notice the presence of left portal vein (*arrowhead*). (**b**) More superior image and (**c**) coronal reformatted image show the small size of left lateral segment. (**b**) Notice the left hepatic vein (*arrowhead*)

1.8.5 Hypoplasia of the Left Medial Segment of the Liver

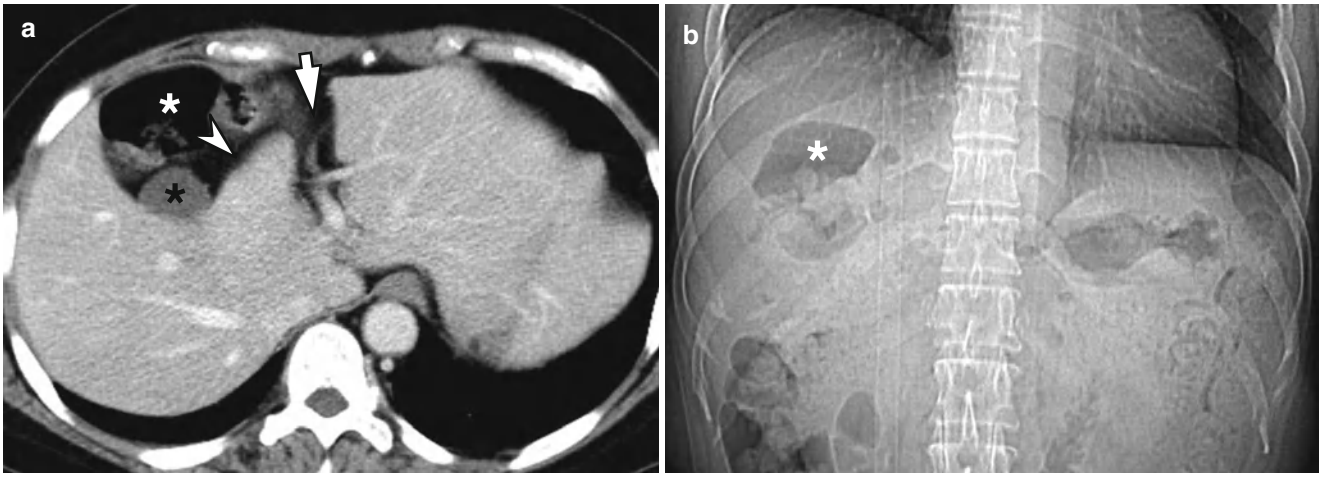

Fig. 1.5 Hypoplasia of the left medial segment of the liver. (**a**) CT shows the small medial segment (*arrowhead*) lying between the fissure for falciform ligament (*arrow*) and gallbladder (*black asterisk*). (**a**, **b**) CT and topogram demonstrate that hepatic flexure colon (*white asterisk*) and omental fat fill the gap created by hypoplasia of the medial segment of the liver

1.8.6 Riedel's Lobe: Ultrasound Findings

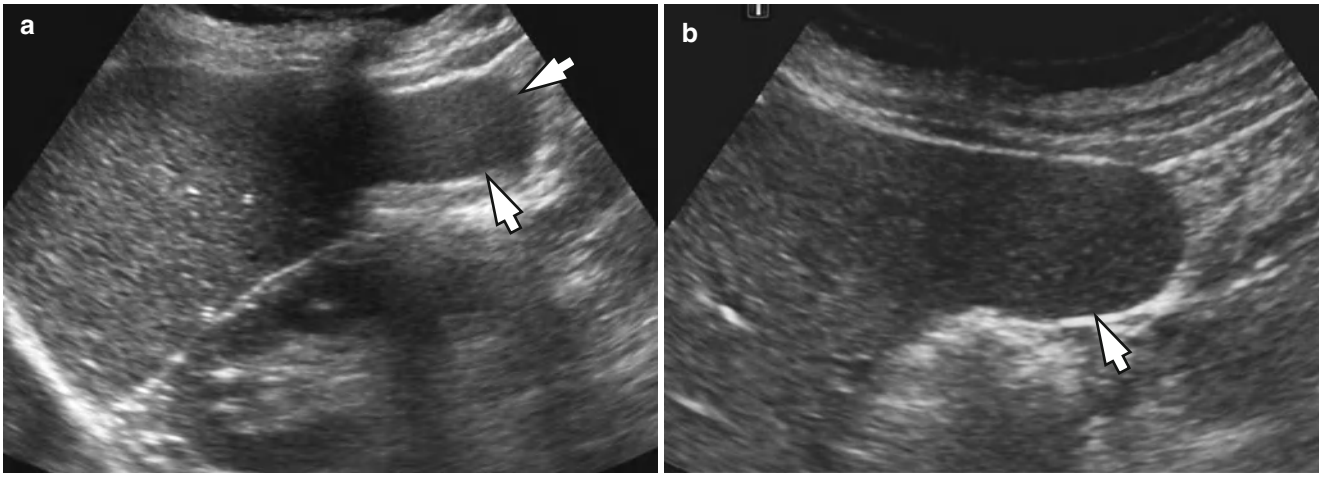

Fig. 1.6 Riedel's lobe: ultrasound findings. (**a**) Ultrasound image which is scanned in an oblique coronal plane shows soft tissue (*arrows*) anterior to the right kidney. (**b**) Ultrasound image on a different plane in the same individual reveals elongation of the right lobe (Riedel's lobe) (*arrow*) which shows same echogenic texture with the other part of the liver

1.8.7 Riedel's Lobe: CT Findings

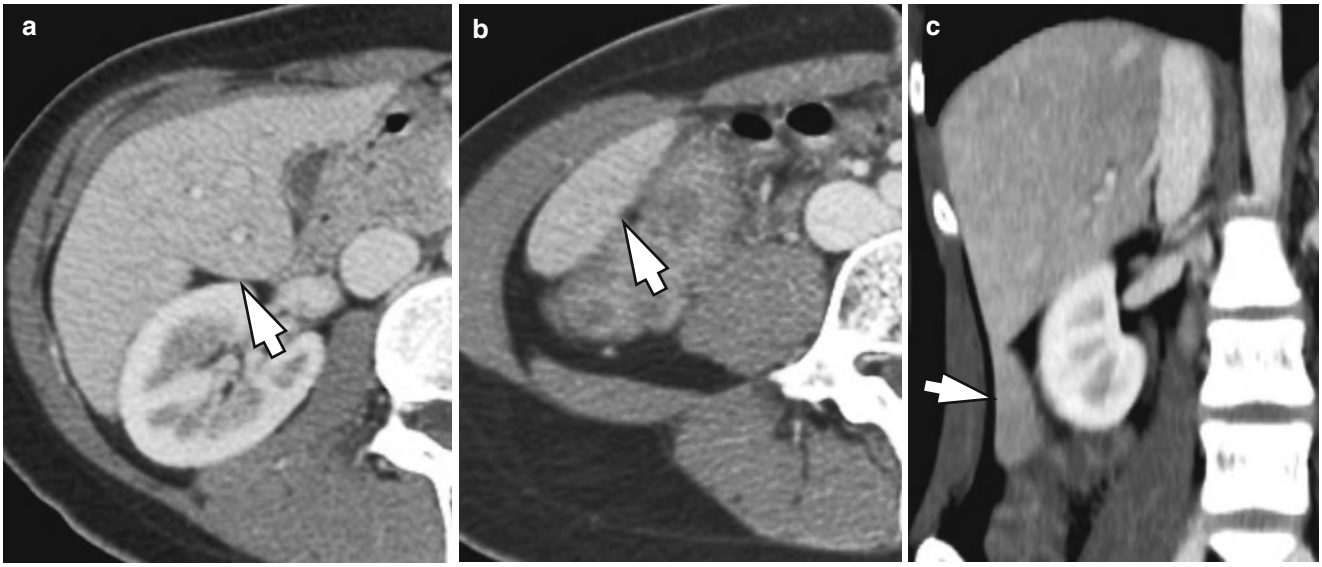

Fig. 1.7 Riedel's lobe: CT findings. (**a**, **b**) Axial CT images in a 28-year-old female show the inferior extension of the liver parenchyma (*arrows*) from the anterior portion of the right lobe which is located anteriorly to the right kidney and along the right paracolic gutter. (**c**) Coronal reformatted CT image demonstrates the tongue-like downward elongation of the hepatic parenchyma (*arrow*), which is consistent with Riedel's lobe

1.8.8 Accessory Lobe of the Liver with Mass

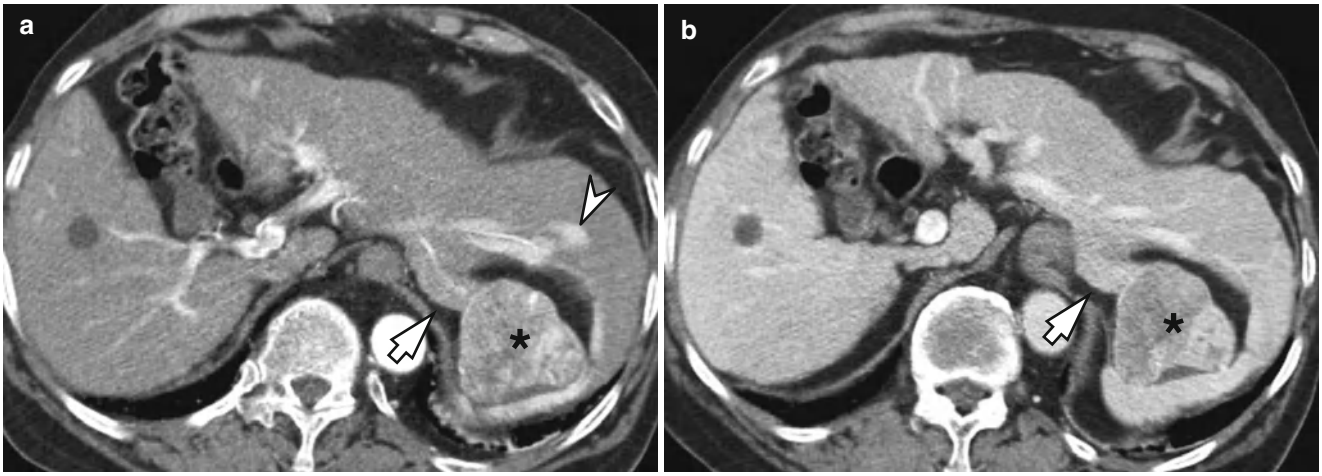

Fig. 1.8 Accessory lobe of the liver with mass. (**a**) Arterial and (**b**) portal phase CT images of a 78-year-old female show hepatocellular carcinoma (*asterisks*) in the accessory hepatic lobe (*arrows*) which is attached to the left lateral superior segment (segment II). Portovenous shunt is detected in the segment II (*arrowhead*)

1.8.9 Diaphragmatic Slips: CT Findings

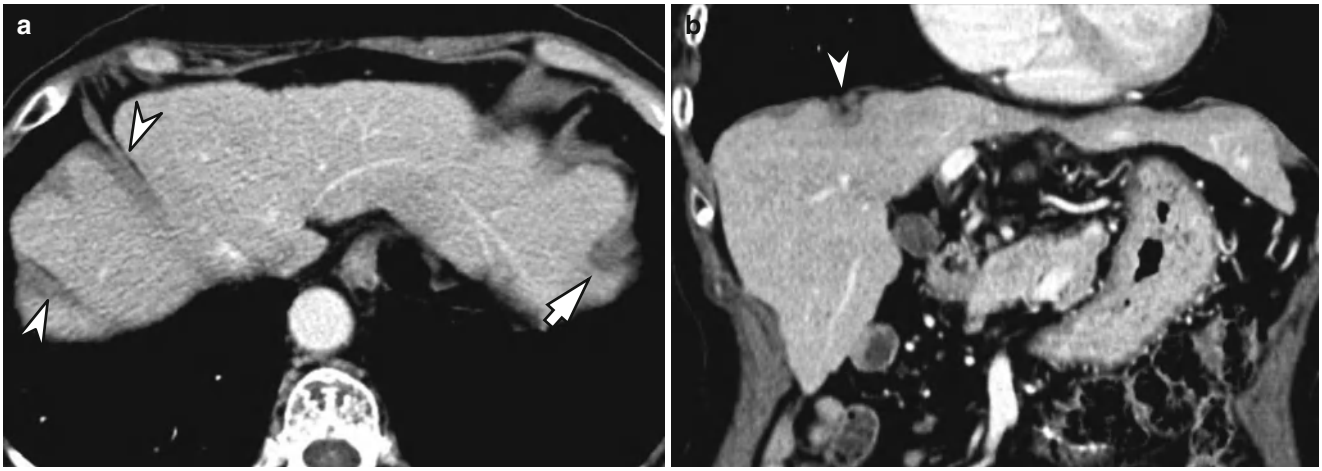

Fig. 1.9 Diaphragmatic slips: CT findings. (**a**) Axial and (**b**) coronal CT images in a 60-year-old female demonstrate the diaphragmatic invaginations (*arrow* and *arrowheads*) in the superior aspect of the liver which result in pseudoaccessory fissures, "diaphragmatic slips." Diaphragmatic slips can be seen as nodular density (*arrow*) in some sections of CT images; therefore, it may mimic hepatic nodule

1.8.10 Diaphragmatic Slips: Radiography and Ultrasound Findings

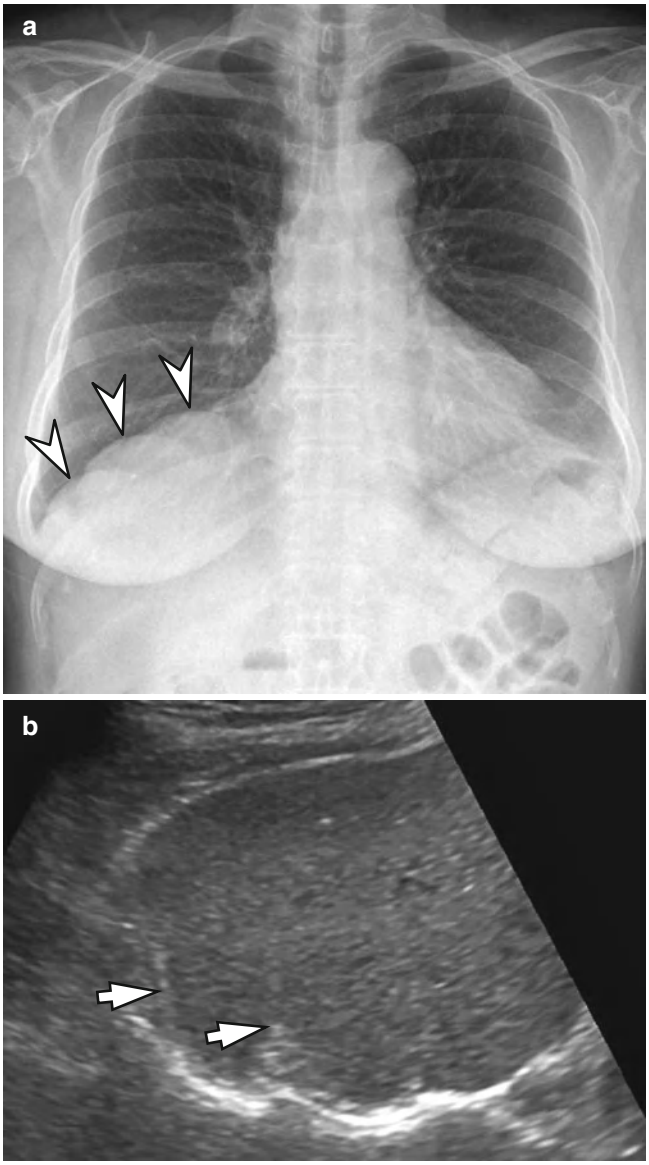

Fig. 1.10 Diaphragmatic slips: radiography and ultrasound findings. (**a**) Diaphragmatic invagination in the liver causes lobulated soft tissue densities (*arrowheads*) along the right diaphragm on the chest radiography. These findings can be mistaken for soft tissue masses in the lung or pleura. (**b**) Ultrasound image in the same patient shows lobulation of the liver surface as well as echogenic lines (*arrows*) which are consistent with diaphragmatic slips

1.8.11 Accessory Fissure of the Liver

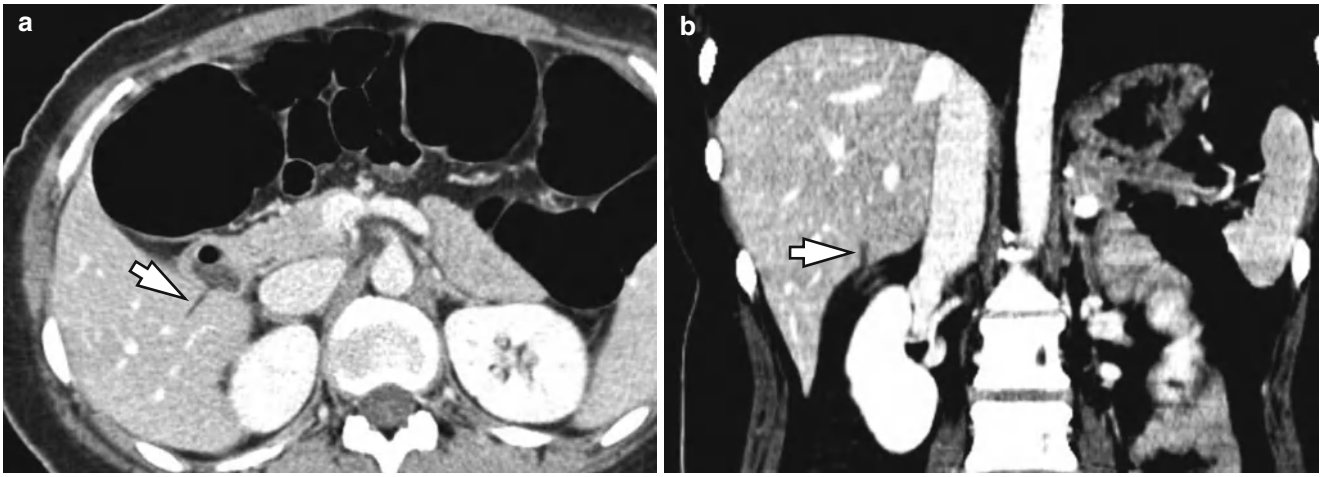

Fig. 1.11 Accessory fissure of the liver. (**a**) Axial and (**b**) coronal CT images in a 37-year-old female show incidentally detected accessory fissure (*arrows*) of the liver which is located in the inferior surface of the right hepatic lobe

1.8.12 Accessory Fissure of the Liver with Loculated Fluid Collection

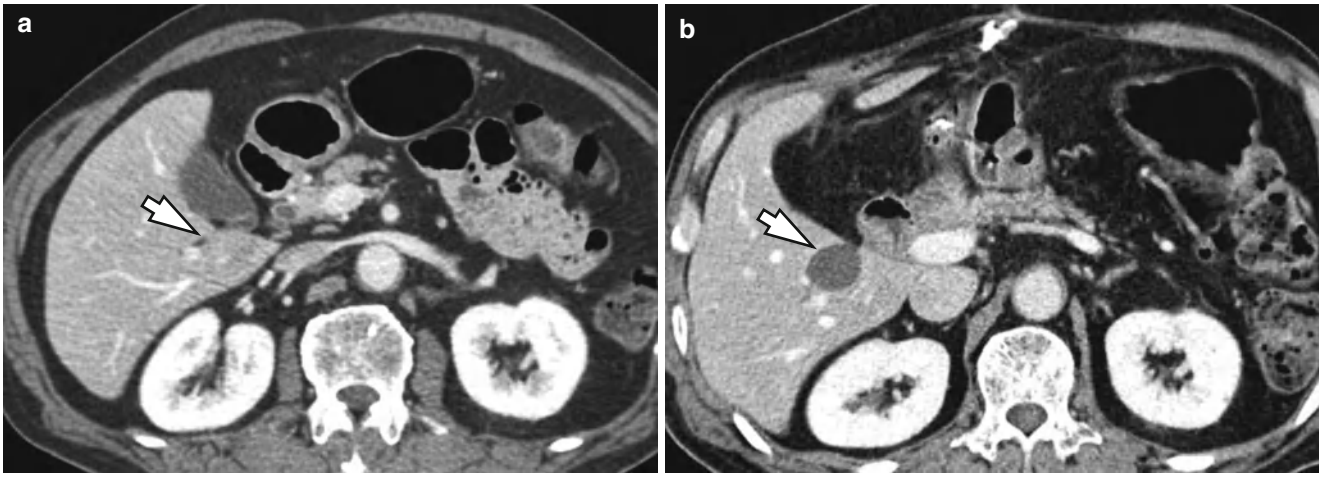

Fig. 1.12 Accessory fissure of the liver with loculated fluid collection. (**a**) Preoperative CT image revealed slit-like accessory fissure (*arrow*) in the right hepatic lobe. (**b**) CT scan after pylorus-preserving pancreaticoduodenectomy in the same patient shows loculated ascites (*arrow*) in the accessory fissure of the liver

1.8.13 Sliver of the Liver

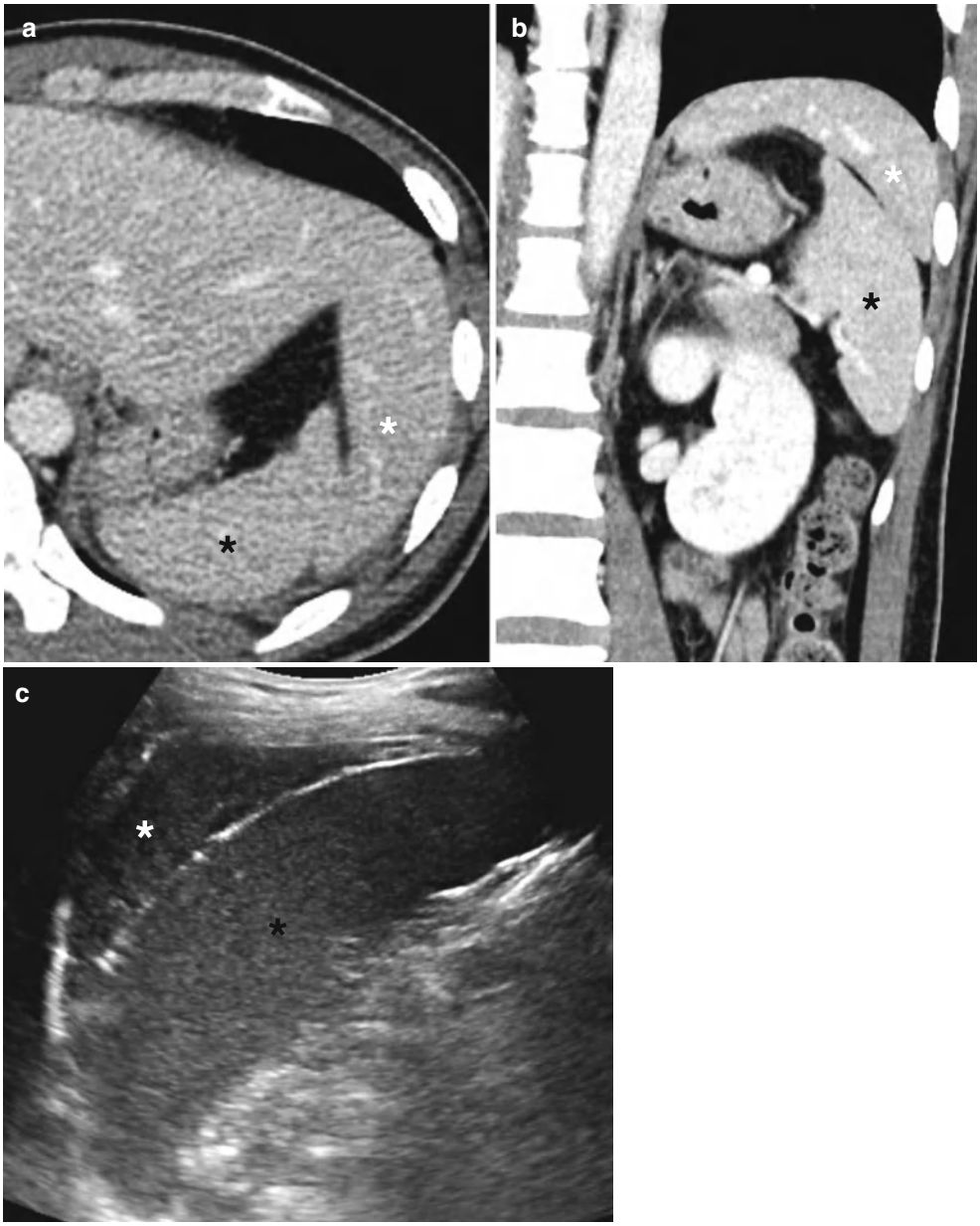

Fig. 1.13 Sliver of the liver. (**a**) Axial and (**b**) coronal CT images show the leftward extension of the left lobe of the liver (*white asterisks*) wrapping the spleen (*black asterisks*), which is a common anatomic variation, "sliver of the liver." (**c**) Ultrasound image in a coronal plane shows the sliver of the liver (*white asterisk*) around the spleen (black asterisk) which may be mistaken for a perisplenic pathologic condition

1.8.14 Papillary Process of the Caudate Lobe

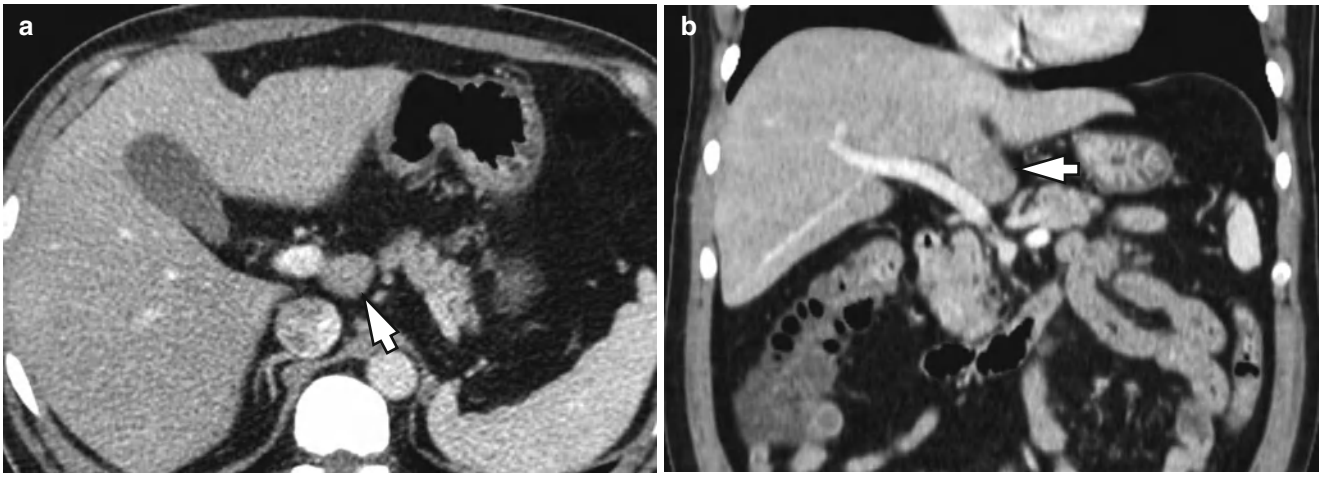

Fig. 1.14 Papillary process of the caudate lobe. (**a**) Axial CT scan at the level of main portal vein shows protruded papillary process of the caudate lobe (*arrow*) which mimics a periportal lymph node or an exophytic pancreatic mass. (**b**) Coronal reformatted CT image reveals the inferior and medial extension of the papillary process of the caudate lobe (*arrow*)

Suggested Reading

Auh YH, Rosen A, Rubenstein WA, et al. CT of the papillary process of the caudate lobe of the liver. AJR Am J Roentgenol. 1984; 142(3):535–8.

Auh YH, Rubenstein WA, Zirinsky K, et al. Accessory fissures of the liver: CT and sonographic appearance. AJR Am J Roentgenol. 1984; 143(3):565–72.

Auh YH, Lim JH, Kim KW, et al. Loculated fluid collections in hepatic fissures and recesses: CT appearance and potential pitfalls. Radiographics. 1994;14(3):529–40.

Dachman AH. Anomalies and anatomic variants of the spleen. In: Gore RM, Levine MS, editors. Textbook of gastrointestinal radiology. 3rd ed. Philadelphia: Saunders; 2008.

Gallego C, Velasco M, Marcuello P, et al. Congenital and acquired anomalies of the portal venous system. Radiographics. 2002; 22(1):141–59.

Kudo M. Riedel's lobe of the liver and its clinical implication. Intern Med. 2000;39(2):87–8.

Kostov DV, Kobakov GL. Accessory hepatic lobe. Surg Radiol Anat. 2011;33(9):819–22.

Watson JR, Lee RE. Accessory lobe of the liver with Infarction. Arch Surg. 1964;88:490–3.

Diffuse Liver Disease

2

Jeong Hee Yoon and Jeong Min Lee

Contents

J.H. Yoon • J.M. Lee (✉)
Department of Radiology, Seoul National University Hospital,
Seoul, Republic of South Korea
e-mail: jhjhry@gmail.com; jmsh@snu.ac.kr,
jmlshy2000@gmail.com

B.I. Choi (ed.), *Radiology Illustrated: Hepatobiliary and Pancreatic Radiology*, Radiology Illustrated,
DOI 10.1007/978-3-642-35825-8_2, © Springer-Verlag Berlin Heidelberg 2014

Table 2.1 Diffuse liver disease depends on radiologic finding

Attenuation change	
Low attenuation	Fatty liver, steatohepatitis
High attenuation	Amiodarone, hemosiderosis, hemochromatosis, GSD, chronic arsenic poisoning, gold therapy, Wilson's disease, shock liver
Heterogeneous attenuation	Uneven fatty liver, radiation hepatitis, sinusoidal obstruction syndrome
Morphologic change	
Enlarged	Acute hepatitis, alcoholic hepatitis, hematologic disease (lymphoma, leukemia), metabolic disease (Wilson's disease, GSD)
Shrunk	Chronic hepatitis, liver cirrhosis, end stage of metabolic disease (Wilson's disease, GSD)
Contour deformity	Liver cirrhosis, pseudocirrhosis by tumor, PVT change
Multifocal hepatic lesions	
Hypervascular	Multinodular HCC, diffuse hypervascular metastasis, focal nodular hyperplasia/nodular regenerating hyperplasia, peliosis, AP shunt
Hypovascular	Multiple regenerative nodules/dysplastic nodules, diffuse hypovascular metastasis, multiple myeloma, lymphoma, leukemia, sarcoidosis, candidiasis, eosinophilic abscess, extramedullary hematopoiesis (rare)
Hypovascular, cystic	Biliary hamartoma, ADPKD, cystic metastasis
Other	Multiple fat deposition

Note: *GSD* glycogen storage disease, *PVT* portal vein thrombosis, *HCC* hepatocellular carcinoma, *AP shunt* arterioportal shunt, *ADPKD* autosomal dominant polycystic kidney disease

Since diffuse liver disease usually represents alternation of its metabolic pathway, cross sectional imaging studies may play a limited role in evaluating diffuse liver disease whereas they are crucial for detection and characterization of focal liver lesions. However, owing to imaging technology advances and use of tissue-specific contrast agents ultrasound (US), computed tomography (CT), and magnetic resonance (MR) imaging have been more frequently used for diagnosis of diffuse liver disease, determining the causes of the diffuse liver disease, assessing extent of the disease, and monitoring its progression.

In this chapter, diffuse liver diseases are categorized into three categories based on their radiologic findings: (a) liver parenchymal attenuation changes, (b) morphological changes of the liver contour or size, and (c) multifocal or disseminated liver lesions (Table 2.1).

2.1 Radiologic Modalities

US is the first diagnostic modality of choice for diffuse liver disease. This is routinely performed in patients with predisposing factor of hepatocellular carcinomas (HCCs) for surveillance. It is also performed in patients with liver function test abnormality to exclude the possible biliary obstruction. US is easy to perform and safe to patients with contrast media hypersensitivity or nephropathy. Furthermore, it can avoid radiation hazard. However, US is dependent on operators as well as not an effective diagnostic tool for obese patients due to poor sonic window. On US, operators usually compare the echogenicity of the liver with that of right kidney to detect the presence of fatty liver. Increased echogenicity on US, however, is seen in not only fatty liver but also other types of diffuse liver diseases.

CT is commonly used for evaluation of both focal and diffuse liver diseases. Non-contrast CT scan is useful for diagnosing fatty liver and hemochromatosis by comparing liver attenuation with splenic attenuation. On contrast-enhanced CT scans, the size and contour of the liver are easily assessed. With respect to diffuse liver diseases manifested as multifocal liver lesions, CT is a powerful tool for detection, characterization, and monitoring of those focal liver lesions. CT also has an advantage of surrounding organ evaluation. Owing to recent advances of CT techniques, high-resolution images can be achieved within a short time with lower radiation dose than before.

MR imaging has also been used for evaluating various hepatic diseases since breath-hold imaging acquisition sequences and hepatocyte-specific contrast agents were developed. MR plays an important role for focal liver lesion evaluation, but recently it draws a lot of attention as an effective tool for evaluation of diffuse liver disease by virtue of its chemical shift imaging (CSI), MR spectroscopy, diffusion weighted imaging (DWI) and MR elastography (MRE). In addition, T2-weighted image (WI) and T2*-WI are useful for evaluation of hemochromatosis. The advent of hepatocyte-specific contrast agent (Gd-EOB-DTPA) helps in the evaluation of liver disease by providing hepatobiliary phase imaging. Recently, there have been attempts to predict liver function using Gd-EOB-DPTA enhanced MRI as well.

Elastography is a tissue stiffness imaging, based on US or MR by measuring speed of sound across the tissue after vibrating a tissue. Instead of palpation for superficial organs, US based elastography (USE) such as transient elastography (TE), shear-wave elastography (SWE), acoustic radiation force impulse (ARFI) imaging, and MR elastography (MRE) are used for liver stiffness measurement. In MRE, mechanical waves are transmitted into the liver, and tissue stiffness is calculated by analyzing the propagation of shear waves using a motion-sensitive MR pulse sequence. In SWE, shear wave generated by push pulses from US probe is captured and tissue stiffness is calculated by measuring shear wave velocity. Liver stiffness values increase in advanced fibrosis. Since fibrosis itself is not clearly depicted on conventional imaging, elastography draws a lot of attention for fibrosis evaluation in the liver.

2.2 Radiologic Findings

2.2.1 Attenuation/Signal Intensity Changes of the Liver Parenchyma

2.2.1.1 Fatty Liver

Fatty liver disease comprises a spectrum of conditions including simple hepatic steatosis and steatohepatitis of